A. DI GERLANDO, R. PERINI

ENERGY SAVING IMPROVED EVALUATION OF INVERTER UPGRADE IN SUBMERSIBLE PUMP INDUCTION MOTOR DRIVES

Proceedings of the International Symposium on Power Electronics, Electrical Drives, Automation and Motion
SPEEDAM 2000

June 13-16, 2000
Ischia, Italy

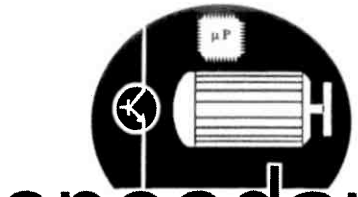

speedam 2000

Symposium on

POWER ELECTRONICS

ELECTRICAL DRIVES

AUTOMATION & MOTION

PROCEEDINGS

June, 13th - 16th 2000

ISCHIA (Italy)

speedam
13-16 June 2000
Ischia (Italy)

Symposium on
POWER ELECTRONICS, ELECTRICAL DRIVES, AUTOMATION & MOTION

Energy Saving Improved Evaluation of Inverter Upgrade in Submersible Pump Induction Motor Drives

Antonino Di Gerlando, Roberto Perini

Dipartimento di Elettrotecnica, Politecnico di Milano - Italy

Abstract

An accurate model of a pumping plant driven by an induction motor is developed, allowing a good estimation of the energy saving achievable with a feeding upgrade, by substituting the mains source with an adjustable-speed inverter feeding, considered all the loss items and the service diagram of the water flow regulation.

1.- INTRODUCTION

In the application sector of the pumping of liquids, where induction motors are generally used, the flow regulation by the speed adjustment is usually considered a convenient solution, compared with the regulation using shutters, inherently energy wasting.

In some previous papers, a few design aspects concerning the motor design and operation optimisation with inverter feeding have been analysed, under the basic assumption of a completely new pumping plant: the degree of freedom of frequency regulation leads to increase the maximum motor speed, reducing the coupled pump size and allowing a good flow regulation [1], [2].

Conversely, the present paper considers an existing pumping plant, with the motor-pump subsystem already installed, with a shutter flow regulation: if a substitution of the motor-pump group is not under consideration, the fundamental questions regard the amount of energy saving and the new operating conditions obtainable with an inverter feeding, taking into account the effective service diagram of the water flow regulation.
These questions are connected with the evaluation of the time-to-recovery of the investment needed for the inverter installation; the following remarks are valid:

- if a wide flow control is operated, the energy lost because of the shutter regulation becomes important, making convenient the inverter installation;
- if the regulation is limited, the energy saved in the pipe may not compensate converter and motor extra losses, making less advantageous the inverter upgrade.

After a description of the system and process models, in the paper the following aspects will be analyzed:

- in case of shutter regulated plants: evaluation of energy savings obtainable by an inverter installation;
- in case of inverter upgraded plants:
  - possibilities of increasing the maximum frequency;
  - evaluation of different motor feeding V(f) laws.

2.- MODELS OF SYSTEM PARTS AND PROCESS

In the following, the models of the different components of the pumping system will be considered, together with the characterisation of the pumping process: in order to achieve realistic quantitative results, reference will be made to a practical plant situation.

2.1- Motor, pump, pipe and shutter

Motor

Depending on the flow regulation technique, the induction motor may be fed directly by the mains or via a converter stage. Considering that the present application does not require particular dynamical performances, the motor can be modelled with the classical T equivalent circuit, valid for the steady state operation at the fundamental components: in the derived admittance, whose applied voltage E takes into account the primary impedance voltage drop, the non-linear core effects are accurately implemented (ferromagnetic saturation - affecting the magnetising current component I_m - and core losses - corresponding to the loss current component I_p -).
About the motor losses, the following must be observed:

- the mechanical loss (weighty, due to the internal water friction) is proportional to the power 2.5 of the speed;
- the stator and rotor I^2R extra losses, due to the

inverter, are negligible (very low current harmonics - thanks to a high switching frequency, without over-modulation - ; weak skin effect - thanks to small diameter stator wires and to limited height rotor bars -);

- the PWM inverter feeding causes extra iron losses, mainly affecting the eddy current item: a simplified correction factor K_{fec} can be used [4]:

$$K_{fec}(m_a) \approx 1 + K_v^2 \cdot (q/m_a - 1) , \quad (1)$$

($K_v \approx 0.75$, $q = 1.47$, m_a inverter modulation ratio).

Table I gives the main data of the chosen motor (corresponding to a real machine; design parameters in [1]).

Table I - Main rated and operating motor data.

Rated voltage and power: V_n [V] ; P_n [kW]	380; 30
number of poles - frequency: p ; f_n [Hz]	2 ; 50
rated efficiency; power factor: η_{mn} [%]; $\cos\varphi_n$	86.6; 0.876
rated slip; air-gap flux density: s_n [%]; $B\delta_n$ [T]	3.2 ; 0.64

Pump

The head-flow characteristics $H_p(Q, N)$ of the plant pump are shown in fig.1, for three different speeds N, together with the pipe characteristics ($H_r(Q)$ = shutter open; $H_r(Q,\rho_A)$ = different shutter regulations).

The power P_p requested at the pump shaft is given by:

$$P_p = g \cdot (\delta_w / k_n) \cdot Q \cdot H_p(Q,N) / \eta_p(Q,N) , \quad (2)$$

where $k_n = 6 \cdot 10^4$ (ℓ/min)/(m³/s), $g = 9.81$ m/s², $\delta_w = 10^3$ kg/m³; P_p depends both on the plant operating point (H,Q) and on the pump efficiency η_p (see fig.2).

The characteristics of fig.s 1, 2 (obtained from experimental curves, measured at a reference speed N_R) have been modelled by cubic spline interpolating functions: $H_{pR}(Q) = H_p(Q,N_R)$, $\eta_{pR}(Q) = \eta_p(Q,N_R)$; called n the p.u. speed ($n = N/N_R$), the curves at the generic N are:

$$H_p(Q,n) = n^2 \cdot H_{pR}(Q/n) , \ \eta_p(Q,n) = \eta_{pR}(Q/n) . \quad (3)$$

Pipe and shutter

The main characteristic of the pipe, together with the general data of the plant are given in Table II: the data of this Table and the pump characteristics have been chosen in such a way that, when the motor of Table I is fed by the mains, it operates near the rated condition.

The pipe is equipped with a motor driven shutter: this flow regulation causes a loss of head, dependent on the flow squared and on the pipe section contraction factor ρ_A (see fig.1: points a1, a2 = shutter regulation, with $0 < \rho_{A2} < \rho_{A1} < 1$ = shutter open; points b1, b2 = speed N regulation; a1,b1 and a2,b2 are at equal flow values Q).

The pipe characteristics is modelled as follows:

$$H_r(Q,\rho_A) = H_g + H_{pr} + H_{dL}(Q) + H_s(Q,\rho_A) , \quad (4)$$

where H_g is the total geodetic head, $H_{pr} = 10.33 \cdot \Delta p$ the output pressure equivalent head, $H_{dL}(Q)$ the pipe distributed head loss (Lang formula) and $H_s(Q,\rho_A)$ the concentrated shutter head loss (Borda formula):

$$H_{dL}(Q) = \alpha \cdot \frac{L}{d^5} \cdot \left[\left(\frac{Q}{k_n} \right)^2 + \beta \cdot \sqrt{\pi \cdot d} \cdot \left(\frac{Q}{k_n} \right)^{1.5} \right] , \quad (5)$$

with $\alpha = 0.16/(\pi^2 \cdot g)$, $\beta = 0.045$;

$$H_s(Q,\rho_A) = \left(\frac{1}{C_c \cdot \rho_A} - 1 \right)^2 \cdot \frac{8 \cdot (Q/k_n)^2}{\pi^2 \cdot d^4 \cdot g} , \quad (6)$$

with $C_c \approx 0.61$ (N.B.: with open shutter: $H_s(Q,1) \approx 0$).

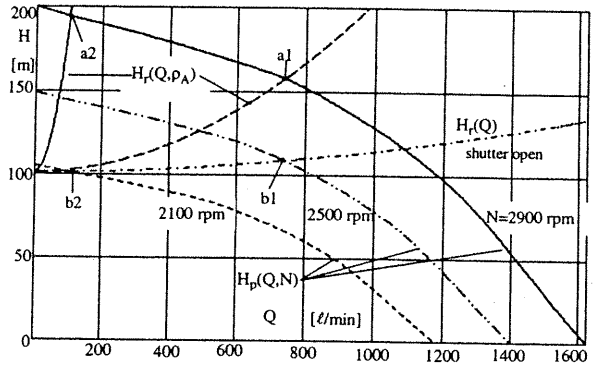

Fig.1 - Head H [m] - water flow Q [ℓ/min] plant curves:
- pump characteristic: $H_p(Q, N)$, with N [rpm] motor speed;
- pipe characteristic: $H_r(Q)$, with shutter open.

Different water flow regulation techniques:
points a1, a2 = constant pump speed, with shutter regulation;
points b1, b2 = variable rotational speed, with shutter open.

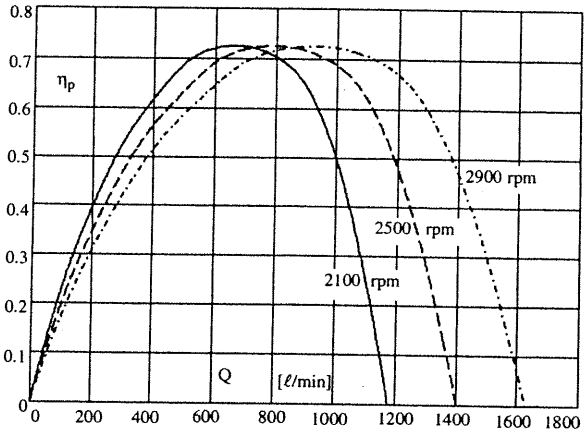

Fig.2 – Efficiency curves of the pump of fig.1.

Table II - General data of the pumping plant

total geodetic height; pipe length: H_g [m]; L [m]	70; 80
pipe diam.; rated water flow: d [mm]; Q_n [ℓ/min]	80; 1000
pipe output pressure increase Δp [atm]	3

2.2- Inverter, rectifier, input transformer

In case of speed adjusted flow regulation, an IGBT PWM VSI inverter is considered, with an input trans-

former feeding a d.c. link capacitor via a diode bridge rectifier: their main data are given in Table III.

Table III - General data of the converter stage components

d.c. link V, switching freq.: V_{dc} [V]; f_s [kHz]	700; 10
IGBT threshold V, differ. res.: V_{ceo} [V]; R_I [mΩ]	1.7; 6.5
rise time, fall time: t_r [μs]; t_f [μs]	0.16; 0.10
free wheel. diode thr.V, diff.R: V_{wo} [V]; R_w [mΩ]	1; 3.5
fr. wheel. d. recov. charge, time: Q_{rr} [μC]; t_{rr} [μs]	34; 0.40
rectifier diode thres.V, diff.R: V_{ro} [V]; R_r [mΩ]	1; 7
transformer rating; sh. circ. voltage: A_n [kVA]; v_k%	50 ; 4
transformer nominal losses: P_{fen} ; P_{cun} [kW]	0.33; 1.1

Table III data allow to analytically estimate inverter losses (cooling ventilation losses, IGBT and free wheeling diode forward losses, switching turn-on and turn-off losses, recovery losses [3]), rectifier losses and input transformer losses, as a function of inverter output voltage V_{out}, current I_{out} and power factor $\cos\varphi_{out}$.

As an example, fig.3 shows the calculated efficiency curves of converter (η_c, rectifier + inverter), transformer (η_t) and global (η_{tc}), for V_{out} = 380 V, $\cos\varphi_{out}$ = 0.85.

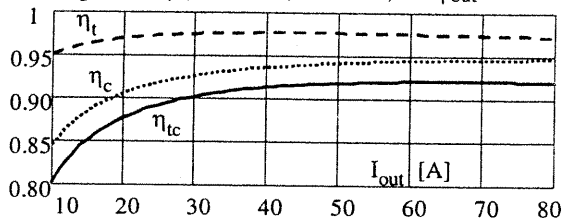

Fig.3 – Converter stage efficiency curves, with V_{out} = 380 V, $\cos\varphi_{out}$ = 0.85 at the inverter output: η_t = input transformer; η_c = converter (inverter + rectifier); $\eta_{tc} = \eta_t \cdot \eta_c$.

The η_{tc} curve shows that, in the rated conditions (I_{out} = 60 A, shutter open), the power absorbed from the mains is higher in case of inverter feeding (with V/f = constant feeding law) than in case of direct mains feeding.

This remark is confirmed by fig.4, showing the input power as a function of Q: $P_{as}(Q)$ is the power absorbed by a shutter regulated plant, while $P_{aIV/f}(Q)$ is that absorbed by the same plant with an inverter feeding (V/f = const.): for comparison needs, the same maximum flow Q_M = 1085 ℓ/min has been considered, as like as the corresponding frequency at the flow Q_M (f_M = 50 Hz).

The following remarks can be made:

- at weak regulation levels, the power absorbed by the inverter driven plant is higher than that requested by the plant directly fed by the mains;
- the lower the flow is, the more important is the energy gap among the two regulation modes, with a higher and higher superiority of the inverter system.

The origin of this energy gap is partially due to the different operating pump efficiencies corresponding to each flow with the two techniques (fig.5). However, this efficiency difference is not sufficient to explain the great power difference of fig.4: the main cause is the power lost in the shutter itself, shown in fig.6 as a function of the flow (via the pipe section regulation factor ρ_A). In fact, the extra power $P_{\ell s}$ requested at the pump output by the shutter, divided by the pump efficiency, corresponds to the extra power at the pump shaft and, finally, to the extra input power, via the electric efficiency.

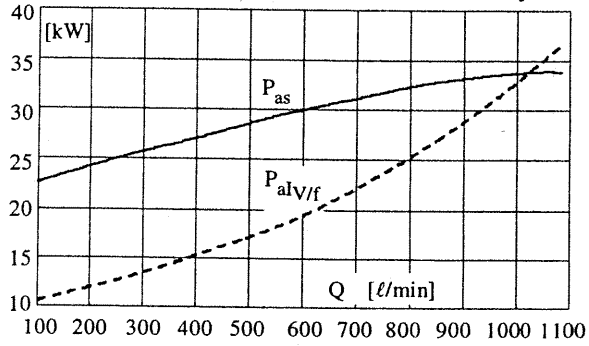

Fig.4 – Power absorbed from the mains by a pumping drive installation, as a function of the water flow regulation:
$P_{as}(Q)$ = power input in case of shutter regulation;
$P_{aIV/f}(Q)$ = power input for V/f = const. inverter feeding law.

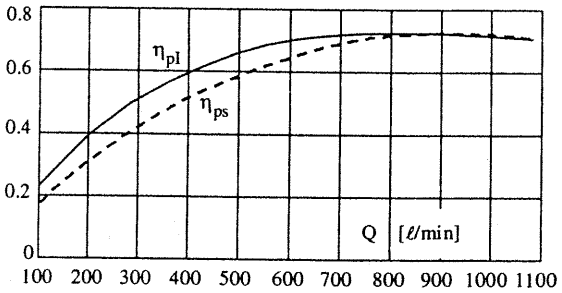

Fig.5 – Pump operating efficiencies occurring at each water flow: $\eta_{ps}(Q)$: shutter regulation; $\eta_{pI}(Q)$: inverter regulation.

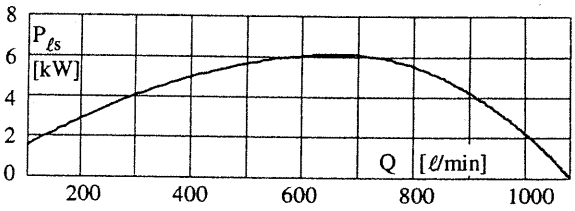

Fig.6 – Hydraulic losses following the shutter, due to the section regulation, for each corresponding operating water flow.

3.- ENERGY SAVINGS WITH INVERTER UPGRADE OF SHUTTER REGULATED PLANTS

3.1- Energetic schematisation of the pumping process

In order to perform energy evaluations it is necessary to consider the time dependence of the requested water flow, and to operate the time integration of the power

quantities of interest. Usually the duty diagram of a pumping plant is known in term of service histogram, linking the p.u. frequencies f to the p.u. water flow values q: in the case of fig.7, the most frequent flow value is around 60% of the maximum (Q_M = 1085 ℓ/min), for roughly 28% of the time: this suggests that the energy saving with a speed regulation can be significant.
Of course, the plant must be sized for the maximum flow Q_M, even if it occurs for less than 5% of time.

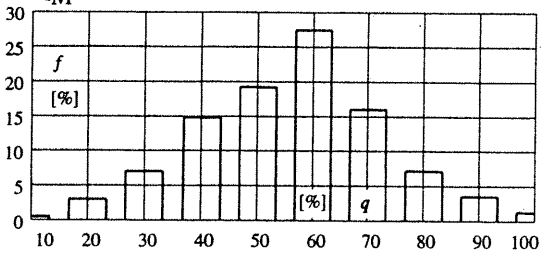

Fig.7 – Pumping plant service diagram histogram: frequencies f of each p.u. flow q referred to the plant maximum flow Q_M.

By operating a fitting manipulation of the histogram data, the parameters of the corresponding Weibull probability density function $f_W(q)$ can be obtained (k_w = shape parameter, c_w = scale parameter):

$$f_W(q) = \frac{k_w}{c_w} \cdot \exp\left[-\left(\frac{q}{c_w}\right)^{k_w}\right] \cdot \left(\frac{q}{c_w}\right)^{(k_w - 1)} \quad . \quad (7)$$

The Weibull function allows to evaluate all the time dependent plant quantities: the matching between the plant service diagram of fig.7 and the power operating characteristics of fig.4 can be obtained by using Weibull function weighted integrals instead of time integrals.
Called: Δt_d the day time duration, Q_{avd} the average daily flow, V_{wd} the daily water volume pumped, W_{adX} the daily absorbed electrical work, being $P_{aX}(q)$ the power absorbed at each p.u. flow q with the "X" flow regulation technique, the following eq.s are valid:

$$Q_{avd} = Q_M \cdot \int_{q_1}^{q_2} q \cdot f_W(q) \cdot dq \; ; \quad V_{wd} = Q_{avd} \cdot \Delta t_d \quad ,(8)$$

$$W_{adX} = \Delta t_d \cdot \int_{q_1}^{q_2} P_{aX}(q) \cdot f_W(q) \cdot dq \quad . \quad (9)$$

These expressions suggest that, being the same the power characteristics, the results of the given integrals greatly depend on the Weibull probability density function, describing in statistical terms the service diagram.

3.2- Energy savings for different service conditions

In Table IV, four service histogram data are considered, different for the regulation range amplitude and distribution: for comparison reasons, the same maximum flow Q_M is supposed; the last two lines give the corresponding Weibull parameters, to be put in (7), and then in (8) and (9). Table V shows the main integral quantities corresponding to the four frequency distributions of Table IV and referred to a duration of one day.

Table IV – Frequencies f of each flow q, with four different pumping plant services (w = wide; m = middle; n = narrow; vn = very narrow); the last two lines give the corresponding Weibull parameters.

Flow	frequency f [%] (x regul. = x regulation)			
q [%]	w regul.	m regul.	n regul.	vn regul.
10	0.5	0.0	0.0	0.0
20	2.9	0.0	0.0	0.0
30	7.1	0.1	0.0	0.0
40	14.8	0.6	0.0	0.0
50	19.2	1.8	0.0	0.0
60	27.4	5.4	0.4	0.0
70	16.0	12.8	2.9	0.0
80	7.2	30.1	16.2	1.7
90	3.5	40.8	49.6	16.9
100	1.3	8.5	30.5	81.3
k_w	3.164	7.708	13.80	26.00
c_w	0.5676	0.8086	0.8956	0.9414

Table V – Daily integral quantities of pumping plant operation, with the four pumping services of Table IV; W_{ad} = energy absorbed from the mains in one day; w_{ad} = specific energy, per one m³ of pumped water; S = Shutter regulation; I = Inverter regulation, with V/f = constant.

Integral quantity	wide range	middle range	narrow range	very narrr. r
average flow [ℓ/min]	584.2	817.8	924.0	990.7
W_{adS} [kWh/day]	695.7	771.4	790.6	801.5
W_{adI} [kWh/day]	450.7	628.3	718.8	781.7
w_{adS} [kWh/m³]	0.881	0.655	0.594	0.562
w_{adI} [kWh/m³]	0.571	0.534	0.540	0.548

The following remarks can be made:
- the daily absorbed energy for a shutter regulation is always higher than that of an inverter V/f regulation;
- the ratio W_{adS}/W_{adI}, high for a wide range (w: 1.54), reduces in the other cases (m: 1.23; n: 1.10; vn: 1.03);
- the difference $W_{adS} - W_{adI}$, significant for the wider ranges, becomes very low for the narrowest ones;
- the comparison among the input energies W_{ad} allows to evaluate the energy savings per day: nevertheless, each diagram implies very different average flows, making non homogeneous the energy comparison;
- the integral quantity most suited to evaluate the energy efficiency of the plant is the specific energy per one m³ of pumped water: in fact, the specific energy for an inverter regulation is practically the same for each

range extension; conversely, the specific energy in case of shutter regulation shows the cited dependence on the range extension.

Thus, in case of narrow or very narrow flow regulation ranges, it is not convenient to substitute the shutter with an inverter, because the energy saving will not compensate the initial investment in a reasonable time period.

4.- SYSTEM PERFORMANCES UNDER DIFFERENT INVERTER FEEDING CONDITIONS

4.1- Possibilities of an increase of the maximum speed

The adoption of an inverter feeding leads to explore the possibility to improve the system performances, by increasing the maximum motor-pump speed; in fact:

- the maximum water flow could be increased;
- a speed increase would imply a better motor cooling;
- a significant motor speed increase has been already achieved (roughly +42%) in case of a completely new installation [1], by reducing the coupled pump size.

A similar analysis, performed in the present situation, led to the conclusion that a significant increase of the maximum speed cannot be obtained: in fact, the presence of the already installed pump (instead of a smaller one) implies an excessive power output requested to the motor, with winding temperatures exceeding the maximum values, even if a better cooling condition occurs.

4.2- Analysis of voltage-frequency feeding laws

During the previous analysis, in case of inverter feeding, the V/f = const. law has been adopted: as known, this law is based on the assumption that the motor operates correctly if the flux is maintained constant.

Nevertheless, considering that the modern inverters allow a digital implementation of the V(f) law, different feeding criteria can be adopted. One interesting law corresponds to the voltage that, for each frequency, minimises the motor losses. The aim of this section is to find this feeding law, comparing it with the classical one, for the conditions of the pumping process here considered.

In the following, all the quantities H regarding the classical V/f = constant law will be identified with the subscript vf (H_{vf}), while those concerning the feeding law at minimum losses will have the subscript mℓ ($H_{m\ell}$).

The main idea of the minimum loss method is based on the following eq. of the gross output power P_{outg} [1]:

$$P_{outg} = P_{outg}(B_\delta, F, s) = \alpha_n \cdot \frac{B_\delta^2 \cdot F^2 \cdot s \cdot (1-s)}{1+(\beta_{rn} \cdot F \cdot s)^2} \qquad (10)$$

with α_n, β_{rn} motor parameters, B_δ air-gap peak flux density, $F = f/f_n$ p.u. frequency and s slip; B_δ, F and s are the fundamental operating variables of the motor.

Considered a frequency value F (to which a value of the speed is approximately associated and, therefore, a value of the power requested by the pump too), the same power P_{outg} can be obtained with different values of air-gap flux density and slip; moreover, the higher the flux density is, the more important the core losses are, and the higher the slip is, the higher the stator and rotor Joule losses are. Thus, for each frequency, a suited choice of slip and of air-gap flux density (dependent on the feeding voltage) allows to obtain the requested power output, with the minimum motor losses.

The results of this analysis are shown in the following.

Fig.8 shows the V(F) functions corresponding to the classical law ($V_{vf}(F)$ = constant·F and to the minimum losses law $V_{m\ell}(F)$, in the frequency range of interest.

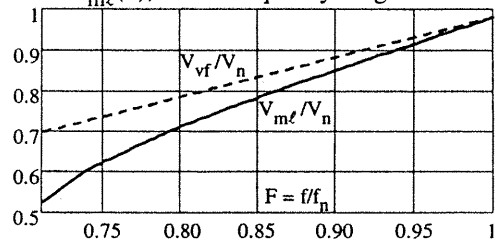

Fig.8 – p.u. feeding laws: classical V/f = constant: $V_{vf}(F)$; minimum losses feeding law: $V_{m\ell}(F)$.

The adoption of the $V_{m\ell}(F)$ implies a flux weakening at low frequencies (see also fig.9, representing the p.u. magnetising current i_m); moreover, as previously discussed, higher slip values occur, as illustrated in fig.10. The loss reduction improves efficiency and power factor (fig.s 11,12), with motor and plant energy advantages.

For each speed, fig.13 shows the ratio of the power $P_{am\ell}$ (absorbed from the mains with $V_{m\ell}(F)$) over the power P_{avf} (absorbed with $V_{vf}(F)$): the energy saving could appear important, especially at low speeds; on the contrary, the effective saving is less significant, because:

- motor operation is already optimised at rated speed;
- the absolute powers absorbed at low speed are small;
- the low speed operation occurs just for a fraction of time, depending on the Weibull frequency diagram.

Table VI shows the energy efficiency obtained for each service of Table IV, with $V_{vf}(F)$ and with $V_{m\ell}(F)$:

$$\eta_{e_{vf}} = W_{out}/W_{a_{vf}} \; ; \; \eta_{e_{m\ell}} = W_{out}/W_{a_{m\ell}} \; . \qquad (11)$$

In (11), while the input work W_a depends on the feeding law, the same value of the output work W_{out} is considered, because plant and service diagram are the same.

As can be observed, only in case of a wide regulation of the flow range, with a significant extension of the service diagram in the low speed interval, an estimable efficiency difference can be obtained ($\Delta\eta_e = 0.5\%$).

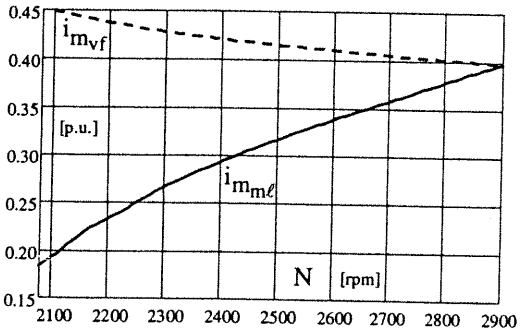

Fig.9 - p.u. magnetizing current, with $V_{vf}(F)$ and $V_{m\ell}(F)$.

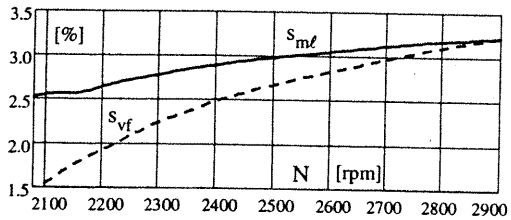

Fig.10 - Slip %, with $V_{vf}(F)$ and $V_{m\ell}(F)$.

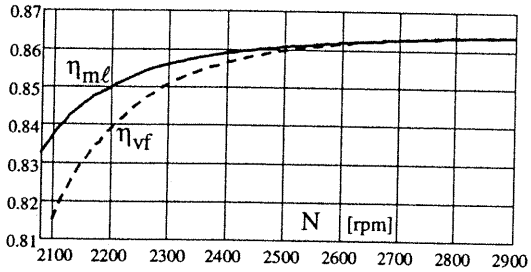

Fig.11 – Motor power efficiency, with $V_{vf}(F)$ and $V_{m\ell}(F)$.

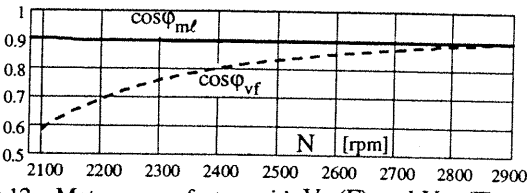

Fig.12 – Motor power factor, with $V_{vf}(F)$ and $V_{m\ell}(F)$.

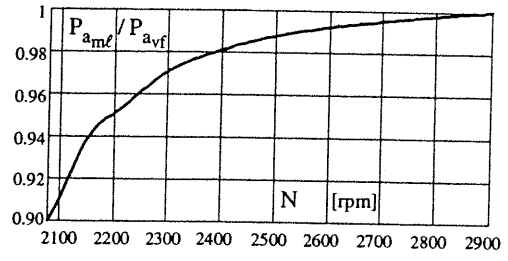

Fig.13 – Plant input powers ratio, with $V_{m\ell}(F)$ and $V_{vf}(F)$.

The conclusion of this analysis is that, in this application and for the considered operating conditions, the V/f = constant law is very near to the feeding law at minimum losses; nevertheless, considering the easy implementation of the $V_{m\ell}(f)$ law in the inverter control board, it could be worth to verify if a "power tuning" of the plant can optimise the system efficiency, by means of off - line tests at different inverter output frequencies.

Table VI – Plant energy efficiency for various flow regulation ranges, with inverter feeding law $V_{vf}(F)$, $V_{m\ell}(F)$.

Energy efficiency: $\eta_e = W_a / W_{out}$	wide range	middle range	narrow range	very narrow ran.
η_e with $V_{vf}(F)$ [%]	76.26	78.52	79.10	79.37
η_e with $V_{m\ell}(F)$ [%]	76.76	78.60	79.12	79.36

5.- CONCLUSIONS

In this paper, an accurate model for the evaluation of the energy savings obtainable in a pumping plant with an induction motor for submersible pump has been developed, considering an inverter upgrade for a speed regulation instead of the direct mains feeding and the water flow regulation by means of a shutter.

The characteristics of the hydraulic components have been accurately developed, together with all the electrical and magnetic phenomena (motor core saturation, inverter, rectifier, input transformer loss items,...) necessary for a comparative estimation: the aim is to evaluate the time-to-recovery of the initial investment required for the inverter installation.

A few service conditions have been considered, by means of a statistical approach, using Weibull functions.

Different feeding laws have been analysed for the inverter operation, showing the level of suitability of the classical V/f = constant law.

REFERENCES

[1] A. Di Gerlando, R. Perini, I. Vistoli, G. Bosi: *Design and Operation Improvements of Inverter Fed Adjustable Speed Induction Motors for Pumping Applications*, Proceedings of ICEM'96, International Conference on Electrical Machines, Vigo, Spain, Sept. 1996.

[2] A. Di Gerlando, R. Perini, I. Vistoli: *Modelling and Design Aspects of Inverter Fed Solid Rotor Submersible Induction Motors for Pumping Drives*; Proceedings of ICEM'98, International Conference on Electrical Machines, Vol.3/3, Istanbul, Turkey, Sept. 1998.

[3] F. Casanellas: *Losses in PWM inverters using IGBTs*, IEE Proc. Electr. Power Appl., Vol.141, N°5, Sept.1994.

[4] A. Di Gerlando, Perini: *Evaluation of the Effects of the Voltage Harmonics on the Extra Iron Losses in the Inverter fed Electromagnetic Devices*, IEEE Transactions on Energy Conversion, Vol.14, N°1, March 1999.